



Original article

Biological aging accelerates hepatic fibrosis: Insights from the NHANES 2017–2020 and genome-wide association study analysis



Jiaxin Zhao^a, Huiying Zhou^a, Rui Wu^a, Chen Ruan^b, Cheng Wang^a, Jiawei Ding^a, Tao Zhang^a, Zheyu Fang^c, Huilin Zheng^d, Lei Zhang^d, Jie Zhou^{e,*}, Zhenhua Hu^{a,e,*}

^a Department of Hepatobiliary and Pancreatic Surgery, Department of Surgery, Fourth Affiliated Hospital, School of Medicine, Zhejiang University, Yiwu, Zhejiang 322000, China

^b Department of Acupuncture, Tongde Hospital of Zhejiang Province, Hangzhou, Zhejiang 310000, China

^c Department of Neurology, The First Affiliated Hospital of Wenzhou Medical University, Wenzhou, Zhejiang 325000, China

^d Zhejiang Provincial Collaborative Innovation Center of Agricultural Biological Resource Biochemical Manufacturing, School of Biological and Chemical Engineering, Zhejiang University of Science and Technology, Hangzhou, Zhejiang 310000, China

^e Department of Hepatobiliary and Pancreatic Surgery, Department of Surgery, First Affiliated Hospital, School of Medicine, Zhejiang University, Hangzhou, Zhejiang 310000, China

ARTICLE INFO

Article History:

Received 16 May 2024

Accepted 21 August 2024

Available online 18 October 2024

Keywords:

NHANES

Mendelian randomization

Phenotypic age

Senescence

Liver fibrosis

ABSTRACT

Introduction and Objectives: This study aimed to investigate the association between biological aging and liver fibrosis in patients with metabolic dysfunction-associated steatotic liver disease (MASLD).

Materials and Methods: We analyzed NHANES 2017–2020 data to calculate phenotypic age. Hepatic steatosis and fibrosis were identified using controlled attenuation parameters (CAP), fatty liver index (FLI) and transient elastography (TE). The odds ratios (ORs) and 95 % confidence intervals (CI) for significant MASLD fibrosis were calculated using multivariate logistic regression, and subgroup analyses were performed. We explored the potential causal relationship between telomere length and liver fibrosis using Mendelian randomization (MR). Additionally, we used the expression quantitative trait loci (eQTL) method and GSE197112 data to identify genes related to liver fibrosis and senescence. Finally, the APOLD1 expression was validated using GSE89632.

Results: Phenotypic age was associated with liver fibrosis occurrence in MASLD (OR = 1.08, 95 % CI 1.05–1.12). Subgroup analyses by BMI and age revealed differences. For obese or young to middle-aged MASLD patients, phenotypic age is significantly associated with liver fibrosis. (OR = 1.14, 95 % CI 1.10–1.18; OR = 1.07, 95 % CI 1.01–1.14 and OR = 1.14, 95 % CI 1.07–1.22). MR revealed a negative association between telomere length and liver fibrosis (IVW method: OR = 0.63288, 95 % CI 0.42498–0.94249). The gene APOLD1 was identified as a potential target through the intersection of the GEO dataset and eQTL genes.

Conclusions: This study emphasized the link between biological aging and fibrosis in young to middle-aged obese MASLD patients. We introduced phenotypic age as a clinical indicator and identified APOLD1 as a potential therapeutic target.

© 2024 Published by Elsevier España, S.L.U. on behalf of Fundación Clínica Médica Sur, A.C. This is an open access article under the CC BY-NC-ND license (<http://creativecommons.org/licenses/by-nc-nd/4.0/>)

Abbreviations: NHANES, national health and nutrition examination survey; MASLD, metabolic dysfunction-associated steatotic liver disease; TE, transient elastography; CAP, controlled attenuation parameters; FLI, fatty liver index; ORs, odds ratios; CI, confidence intervals; MR, Mendelian randomization; eQTL, expression quantitative trait loci; APOLD1, apolipoprotein L domain containing 1; SNPs, single nucleotide polymorphism; GWAS, genome-wide association studies; NCHS, national center for health statistics; FDA, food and drug administration; IQR, interquartile range

* Corresponding authors.

E-mail addresses: jzhou329@zju.edu.cn (J. Zhou), huzhenh@zju.edu.cn (Z. Hu).

<https://doi.org/10.1016/j.aohep.2024.101579>

1665-2681/© 2024 Published by Elsevier España, S.L.U. on behalf of Fundación Clínica Médica Sur, A.C. This is an open access article under the CC BY-NC-ND license (<http://creativecommons.org/licenses/by-nc-nd/4.0/>)

1. Introduction

Non-alcoholic fatty liver disease (NAFLD) is a chronic liver condition, with 17 % to 22 % of patients exhibiting no obvious clinical symptoms. The global prevalence of NAFLD is between 20 % and 30 % [1,2]. Research has shown that various chronic liver diseases may be accompanied by liver fibrosis. Liver fibrosis can progress to cirrhosis or liver cancer, posing a serious threat to human health. Recent advancements in the understanding of this spectrum of liver disorders have led to a paradigm shift in terminology [3]. Specifically, NAFLD has been redefined as MASLD. This updated terminology not only reflects the metabolic foundations of the disease

but also recognizes the varied causes contributing to hepatic steatosis beyond metabolic factors [4]. MASLD can also lead to liver fibrosis, where healthy liver cells are replaced by fibrous tissue. Therefore, timely detection and prevention of the progression of liver fibrosis are crucial in reducing the complications and mortality rates associated with cirrhosis and liver cancer.

Currently, the common causes of liver fibrosis include viral hepatitis, alcohol consumption, metabolic disorders, and exposure to drugs or chemical toxins. Aging is a major risk factor for most chronic diseases, and it may lead to a decline in the regenerative capacity of the liver. The aging of various cells in the liver is critical to the development of liver fibrosis, as aging organs are more prone to fibrosis after injury. This suggests that there is a relationship between age progression and the degree of liver fibrosis [5]. Although aging is a normal biological phenomenon, individuals exhibit variations in the rate of aging. Therefore, besides chronological age, exploring the impact of phenotypic age on liver fibrosis associated with MASLD is crucial.

Phenotypic age, as one of the biological age indicators, is a “phenotypic aging metric” derived from clinical biomarkers and serves as a strong predictor of all-cause mortality [6]. It is calculated based on age and nine clinical biochemical markers, including albumin (g/L), creatinine ($\mu\text{mol/L}$), glucose (mmol/L), C-reactive protein (mg/L), lymphocyte percentage (%), mean cell volume (fL), red cell distribution width (%), alkaline phosphatase (U/L), and white blood cell count (1000 cells/ μL). This parameter was developed using data from the U.S. National Health and Nutrition Examination Survey III (NHANES III) to predict the overall mortality rate [7]. Compared to other predictors of biological aging, the indicators used to assess phenotypic age are more readily available and are pivotal in predicting the incidence and progression of various diseases [8–10]. With advancements in molecular and microscopic-level research, the gradual shortening of telomeres has emerged as one of the hallmarks of aging. Telomeres are chromosome end structures composed of a repeating sequence of six nucleotides 5'-CCCAAAT-3' (complementary strand: 3'-TTGGGGA-5') [11]. Telomere dysfunction serves as an inducer or amplifying

agent of molecular pathways driving aging and related diseases [12].

Mendelian Randomization (MR) is a genetics-based statistical analysis method. It involves examining genetic markers associated with both disease and gene expression simultaneously [13]. When an allele's frequency is higher in cases compared to controls, and it also affects the expression of a nearby gene crucial in the disease, this allows for causal inferences. These markers are typically Single Nucleotide Polymorphisms (SNPs) in regulatory regions that impact gene expression, known as expression quantitative trait loci (eQTLs) [14]. Through the application of MR methods, we can combine information on SNP-gene expression relationships and SNP-disease associations to establish a causal link between exposure and outcome.

In this study, we first used a cross-sectional study to demonstrate that biological aging accelerates the progression of liver fibrosis. We then employed MR to establish a causal relationship between biological aging and liver fibrosis using information on SNP-gene expression relationships and SNP-disease associations. Finally, we validated these findings by intersecting genes identified through transcriptomic analyses with eQTL data to identify target genes.

2. Materials and Methods

2.1. Study design

The study design included a combination of epidemiological observational studies, MR analysis, and transcriptomic analysis, as illustrated in Fig. 1. Initially, we investigated the relationship between phenotypic age and liver fibrosis through epidemiological analyses of NHANES, utilizing subgroup analyses to investigate potential interactions. Following this, we carried out two-sample MR analyses based on GWAS findings to assess causality. We employed various MR methodologies with different modeling assumptions to evaluate the robustness of the results.

Additionally, we integrated data from the GSE197112 liver fibrosis differential gene expression dataset, disease GWAS, and eQTL to

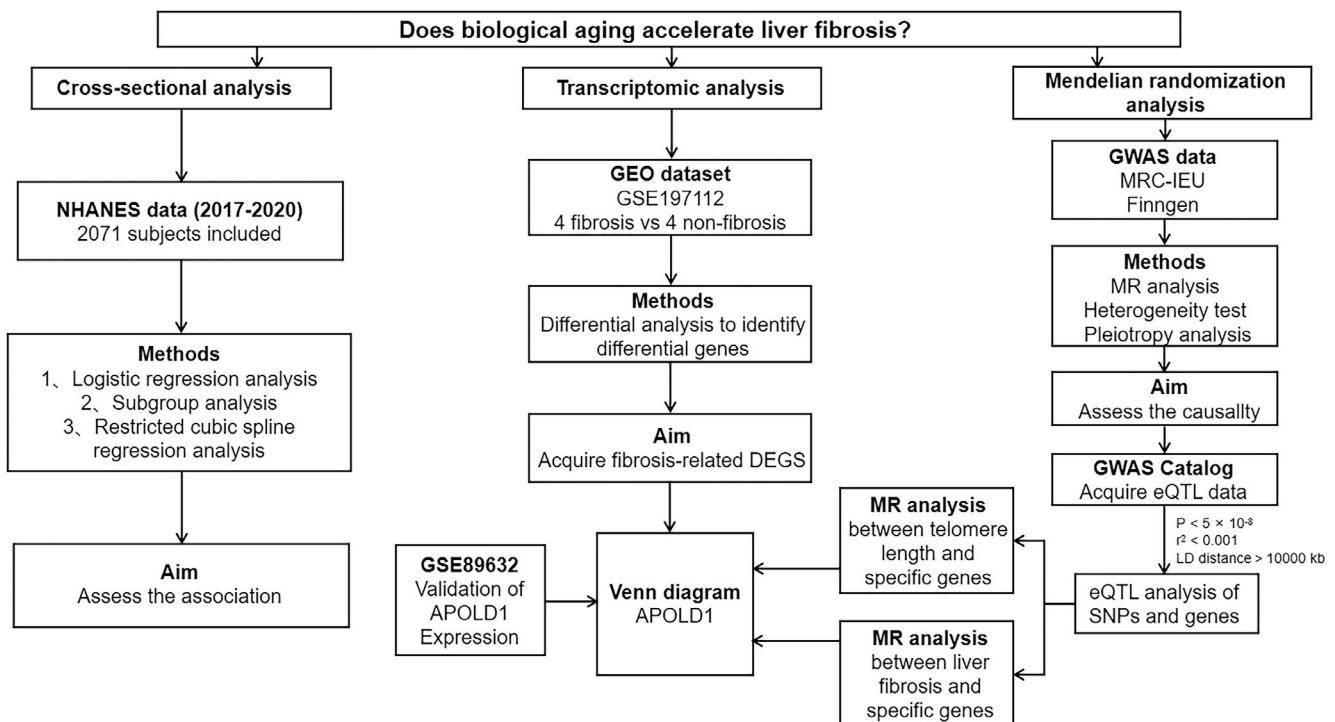


Fig. 1. Flowchart illustrating the present study design.

identify a novel therapeutic target for liver fibrosis and the onset of aging. Validation of the target was performed using the GSE89632.

2.2. NHANES study

2.2.1. Study population

NHANES is a comprehensive survey of the US national population that offers abundant information regarding the health and nutrition of the general public. The data collected from NHANES surveys are publicly accessible, making them a valuable resource for researchers and data users. The NHANES methodology and data collection procedures have been extensively documented in previous publications and are accessible on the official NHANES website (<https://www.cdc.gov/nchs/nhanes.html>). The survey protocol underwent ethical review and approval by the National Center for Health Statistics (NCHS) Research Ethics Review Board, ensuring compliance with ethical standards. Written informed consent was obtained from all participants involved in the study.

We conducted a cross-sectional study using aggregated NHANES data from 2017 to 2020. During that time, a total of 15,561 people participated in the survey. Individuals under 18 years of age were excluded. Transient elastography (TE) is a non-invasive tool for assessing liver fibrosis, while controlled attenuation parameter (CAP) is a promising technology for rapid and standardized quantification of hepatic steatosis. They can be utilized to detect hepatic steatosis and liver fibrosis in populations [15,16]. Fatty Liver Index (FLI) is a calculated method to assess the risk of fatty liver disease by integrating body mass index, waist circumference, levels of triglycerides, and gamma-glutamyl transferase [17]. We used a CAP score ≥ 248 dB/m or Fatty Liver Index (FLI) ≥ 30 to determine the presence of fatty liver disease (i.e., hepatic steatosis) [18,19]. MASLD is defined as the presence of hepatic steatosis and at least one of five cardiometabolic risk

factors (CMRFs): (1) BMI ≥ 23 kg/m² or waist circumference >90 cm (men) or >80 cm (women); (2) fasting serum glucose ≥ 5.6 mmol/L (100 mg/dL), or 2-h post-load glucose ≥ 7.8 mmol/L (≥ 140 mg/dL), or hemoglobin A1c $\geq 5.7\%$ (39 mmol/L), or type 2 diabetes and its treatment; (3) blood pressure $\geq 130/85$ mmHg or specific antihypertensive medication; (4) plasma triglycerides ≥ 1.70 mmol/L (150 mg/dL), or lipid-lowering therapy; (5) plasma HDL cholesterol ≤ 1.0 mmol/L (40 mg/dL) in males, ≤ 1.3 mmol/L (50 mg/dL) in females, or lipid-lowering therapy [20]. The median liver stiffness of 8.2 kPa was used to define cases of significant fibrosis (F2) [21,22], while the control group was defined as MASLD participants without significant fibrosis.

Subjects with missing values for the indicators required to calculate phenotypic age (including age, albumin, creatinine, glucose, C-reactive protein, percentage of lymphocytes, mean red blood cell volume, erythrocyte distribution width, alkaline phosphatase, and white blood cell count), as well as those with calculated phenotypic age at infinity, were excluded from the study. Participants with data on covariates such as viral hepatitis infection (defined as HCV RNA positivity, HCV antibody, or HBsAg positivity), autoimmune hepatitis, hepatocellular carcinoma, excessive alcohol consumption, or lack of smoking status, gender, race/ethnicity, marriage, education, and body mass index (BMI) were further excluded from the analyses. Finally, 2071 patients with MASLD who met the inclusion/exclusion criteria were eligible for analysis (Fig. 2), of whom 255 had significant fibrosis.

2.2.2. Variables

Liver stiffness and steatosis were assessed using TE, CAP and FLI. TE has emerged as a widely adopted, non-invasive, and reproducible technique for assessing liver stiffness in recent years [23]. It has also received approval from the Food and Drug Administration (FDA) to evaluate liver fibrosis. The TE measurements were conducted at the

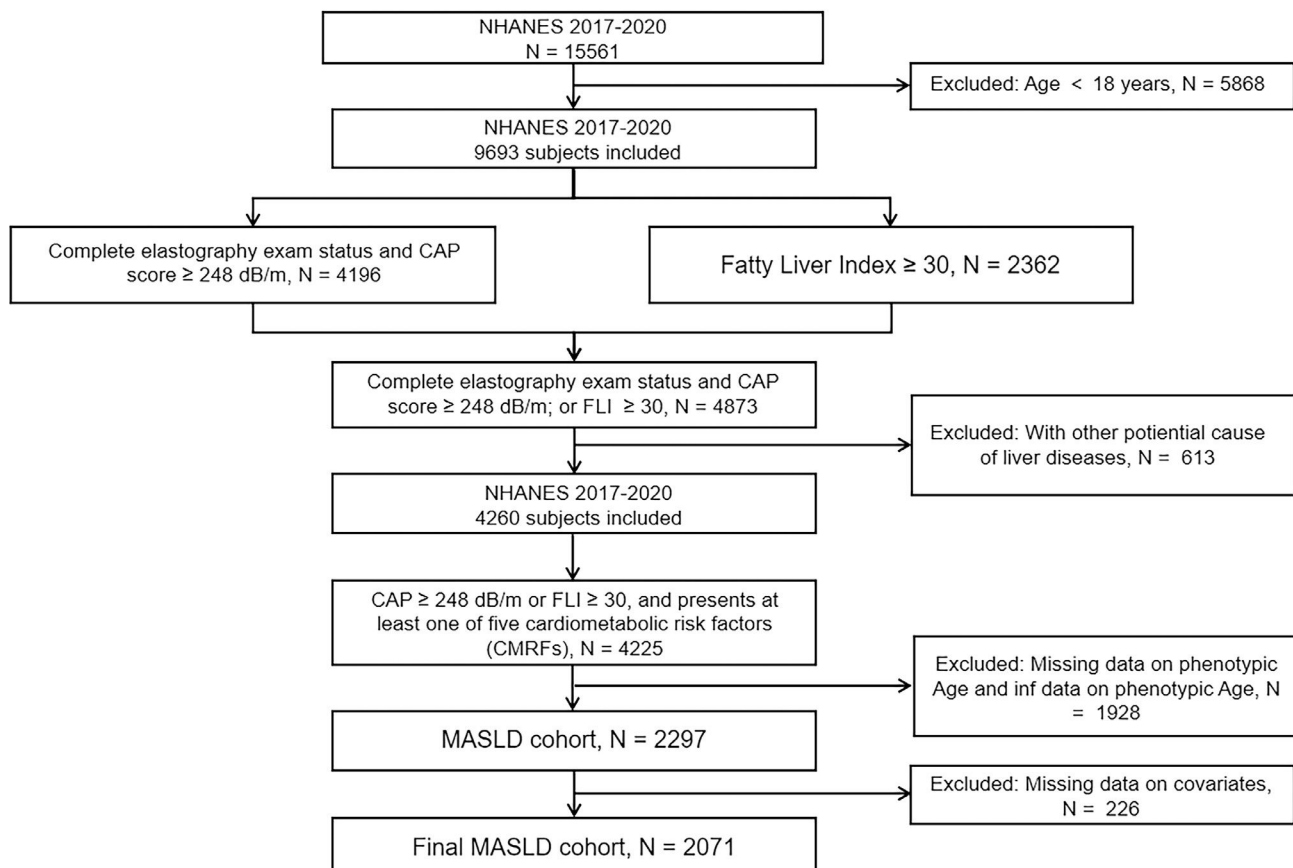


Fig. 2. Flowchart of the sample selection from NHANES 2017–2020.

Table 1
Details of the GWASs analyzed in the present MR analyses.

Phenotype	Consortium	Sample size	Number of variants	Ethnicity	Trait ID in GWAS	Year
Exposure telomere length	MRC-IEU	472,174	20,134,421	European	ieu-b-4879	2021
Outcome Fibrosis and cirrhosis of liver	FinnGen	214,403	16,380,458	European	finn-b-K11_FIBROCHIRLIV	2021

NHANES Mobile Examination Center (MEC) using the FibroScanVR model 502 V2 Touch with either a medium (M) or extra-large (XL) probe. Only participants who underwent complete elastography exams and met criteria such as fasting for at least three hours, obtaining 10 or more valid stiffness measurements, and having a liver stiffness interquartile range/median <30 % were included in the present analysis. FLI is calculated using the formula: $FLI = (e^{(0.953 \times \ln(\text{triglycerides}) + 0.139 \times \text{BMI} + 0.718 \times \ln(\text{GGT}) + 0.053 \times \text{waist circumference} - 15.745)}) / (1 + e^{(0.953 \times \ln(\text{triglycerides}) + 0.139 \times \text{BMI} + 0.718 \times \ln(\text{GGT}) + 0.053 \times \text{waist circumference} - 15.745)}) \times 100$ [17].

We assessed biological aging by calculating the phenotypic age for all included participants in NHANES. This included age, albumin, alkaline phosphatase, creatinine, glucose, and C-reactive protein concentrations, lymphocyte percentage (i.e., the proportion of leukocytes accounted for by lymphocytes), mean cell volume, erythrocyte distribution width, and leukocyte count. The following formula was used to ascertain the phenotypic age:

$$xb = -19.90667 + (-0.03359355 \times \text{albumin}) + (0.009506491 \times \text{creatinine}) + (0.1953192 \times \text{glucose}) + (0.09536762 \times \text{C-reactive protein}) + (-0.01199984 \times \text{lymphocyte percentage}) + (0.02676401 \times \text{mean cell volume}) + (0.3306156 \times \text{erythrocyte distribution width}) + (0.001868778 \times \text{alkaline phosphatase}) + (0.05542406 \times \text{leukocyte count}) + (0.08035356 \times \text{age})$$

$$\text{orig} = 1 - (\exp((-1.51714 \times \exp(xb))) / 0.007692696))$$

$$\text{Phenotypic Age} = ((\log(-0.0055305 \times (\log(1 - \text{orig}))) / 0.09165) + 141.50225)$$

$$\text{PhenoAgeAccel} = \text{Phenotypic Age} - \text{Chronological Age}.$$

Zuyun Liu et al. introduced the concept of phenotypic age acceleration to distinguish between an individual's chronological age and their phenotypic age difference. The metric, denoted as phenotypic age acceleration (PhenoAgeAccel), is calculated as the difference between phenotypic age and chronological age. Phenotypic aging is defined as a condition where PhenoAgeAccel is greater than 0, while phenotypic rejuvenation occurs when PhenoAgeAccel is less than or equal to 0 [8].

We included several categorical variables as covariates in our analyses, namely sex, race/ethnicity, education level (less than high school vs. more than high school), marital status, smoking status, BMI and recreational physical activity. Additionally, continuous covariates age and alcohol consumption were incorporated into our analyses. Participants were queried about their lifetime smoking history, current smoking habits, and alcohol consumption using two 24-h recalls. Former smokers were identified as individuals who had smoked 100 cigarettes in the past but were not currently smoking. Excessive alcohol consumption was defined as an average of >30 g/day for men and >20 g/day for women [24]. In cases where two 24-h recalls were completed, the average alcohol intake from both recalls was utilized. Otherwise, data from the first 24-h recall was used. The measured BMI was categorized into four groups: underweight, normal, overweight, or obese (<18.5, 18.5–25, 25–29.9, ≥30 kg/m², respectively).

2.2.3. Statistical methods

Our study followed NHANES sampling procedures and applied complex survey weights for national representativeness. We

evaluated the prevalence of fibrosis in MASLD participants. Descriptive statistics summarize data as follows: mean ± standard deviation (SD) for normally distributed continuous variables, median (IQR) for skewed variables, and frequency (%) for categorical variables. Logistic regression models assessed the relationship between PhenoAgeAccel and liver fibrosis, treating phenotypic age as both continuous and dichotomous in the models. Weighted logistic regression included unadjusted Model 1, adjusted Model 2 (age, sex, race, and marital status), and fully adjusted Model 3. Restricted cubic spline regression was used to explore the relationship between phenotypic age and liver fibrosis onset. Subgroup analyses by sex, BMI, and age were conducted. Statistical analysis was conducted using R 4.2.1, with significance set at $P < 0.05$.

2.3. Mendelian randomization analysis

2.3.1. Data access

The genetic data for telomere length was sourced from the MRC-IEU database, while the data for fibrosis and cirrhosis of the liver was obtained from the FinnGen database. All the data originated from European populations. The details of the collected data can be found in Table 1. To identify SNPs strongly linked to telomere length, we established statistical significance thresholds ($P < 5 \times 10^{-8}$) and considered linkage disequilibrium (LD) with an $r^2 < 0.001$ and an LD distance $> 1 \times 10^4$ kb. The F -statistic was employed to evaluate the strength of the relationship between a SNP and telomere length. SNPs with an F -value exceeding 10 are generally considered to be significantly associated with telomere length.

The eQTL data utilized in this study were sourced from the eQTL-Gen Consortium (<https://eqtlgen.org/>). Specifically, the eQTLGen dataset comprises information on 16,987 genes and 31,684 cis-eQTLs identified in blood samples primarily collected from healthy individuals of European descent. For a comprehensive overview of the dataset, readers are encouraged to refer to the original publication [25]. To identify genetic variants associated with gene expression, we conducted eQTL analysis using data obtained from the GWAS Catalog website (<https://gwas.mrcieu.ac.uk/>). We employed the R package “TwoSampleMR” to identify SNPs strongly correlated with gene expression as instrumental variables.

2.3.2. Mendelian randomization study design

We employed SNPs that were significantly associated with telomere length as instrumental variables (IVs) while using fibrosis and cirrhosis of the liver as the outcome variables. We took several steps to ensure the validity of our causal analysis, including excluding outliers from the dataset and conducting a two-sample MR analysis with tests for heterogeneity and multiple validity. We also performed sensitivity analyses to confirm the reliability of our results.

The use of IVs in MR studies relies on three key assumptions: (1) IVs should be strongly correlated with the exposure factors; (2) IVs should only affect the outcome through the exposure factors and not directly; and (3) IVs should not be related to any confounding factors that could influence the association between the exposure and outcome.

We estimated causal effects primarily using the inverse variance weighting (IVW) method, supplemented by MR-Egger regression, weighted multinomial (WM), and weighted median (WME) methods. These methods involve clustering SNPs into subsets based on their

Table 2
Characteristics of participants with MASLD by significant liver fibrosis status in the 2017–2020 NHANES.

Characteristic	Overall, N = 2071	liver fibrosis		P Value
		No, N = 1816	Yes, N = 255	
Age (median [IQR])	52.0 (37.0, 64.0)	52.0 (37.0, 64.0)	54.0 (42.7, 66.0)	0.034
Sex (%)				>0.9
male	1046 (53 %)	909 (53 %)	137 (53 %)	
female	1025 (47 %)	907 (47 %)	118 (47 %)	
Race (%)				0.4
Mexican American	300 (9.9 %)	259 (9.9 %)	41 (9.9 %)	
Other Hispanic	234 (7.6 %)	210 (7.8 %)	24 (6.2 %)	
Non-Hispanic White	713 (62 %)	607 (62 %)	106 (69 %)	
Non-Hispanic Black	512 (11 %)	456 (11 %)	56 (8.8 %)	
Non-Hispanic Asian	203 (4.6 %)	186 (4.7 %)	17 (3.6 %)	
Other Race - Including Multi-Racial	109 (4.5 %)	98 (4.7 %)	11 (2.9 %)	
Marital status (%)				0.3
Married/Living with Partner	1266 (65 %)	1107 (65 %)	159 (68 %)	
Widowed/Divorced/Separated	479 (20 %)	417 (20 %)	62 (20 %)	
Never married	326 (15 %)	292 (15 %)	34 (12 %)	
Education level (%)				0.5
≤High school	414 (12 %)	365 (12 %)	49 (13 %)	
>High school	1657 (88 %)	1451 (88 %)	206 (87 %)	
BMI (%)				<0.001
Underweight (<18.5 kg/m ²)	3 (0.2 %)	3 (0.2 %)	0 (0 %)	
Normal (18.5 kg/m ² to <25 kg/m ²)	195 (8.6 %)	185 (9.2 %)	10 (3.9 %)	
Overweight (25 kg/m ² to <30 kg/m ²)	678 (33 %)	647 (36 %)	31 (11 %)	
Obese (30 kg/m ² or greater)	1195 (58 %)	981 (54 %)	214 (85 %)	
Smoking (%)				0.6
Current smoker	318 (13 %)	285 (14 %)	33 (12 %)	
Former smoker	551 (28 %)	468 (28 %)	83 (32 %)	
Never smoker	1202 (58 %)	1063 (59 %)	139 (56 %)	
Alcohol consumption (%)				0.13
0 (g/day)	1698 (78 %)	1476 (77 %)	222 (88 %)	
1–10 (g/day)	162 (8.7 %)	147 (9.2 %)	15 (4.9 %)	
10–20 (g/day)	149 (8.2 %)	136 (8.6 %)	13 (4.9 %)	
20–30 (g/day)	62 (4.8 %)	57 (5.1 %)	5 (2.5 %)	
Vigorous recreational activities (%)	942 (53 %)	844 (54 %)	98 (45 %)	0.033
FLI (median [IQR])	71.6 (47.0, 90.9)	67.7 (44.5, 88.0)	95.3 (85.4, 98.7)	<0.001
Median controlled attenuated parameter (median [IQR])	287 (255, 329)	281 (251, 320)	338 (298, 378)	<0.001
Median liver stiffness (median [IQR])	5.20 (4.30, 6.50)	5.00 (4.10, 5.90)	10.88 (8.90, 14.55)	<0.001
Phenotypic Age (median [IQR])	52.9 (38.9, 65.8)	51.7 (37.7, 65.2)	58.7 (48.1, 70.6)	<0.001
PhenoageAccel (median [IQR])	0.5 (−2.9, 5.0)	0.1 (−3.1, 4.5)	3.9 (0.2, 9.0)	<0.001
PhenoageAccel (%)				<0.001
≤0 years	872.0 (46.1 %)	820.0 (49.2 %)	52.0 (22.9 %)	
>0 years	1199.0 (53.9 %)	996.0 (50.8 %)	203.0 (77.1 %)	

causal effects and estimating the causal effect of the subset with the largest number of SNPs. To assess heterogeneity, we conducted Cochran's Q and Rücker's Q tests using IVW and MR-Egger methods. We also performed multiplicity testing using the intercept term of MR-Egger regression and sensitivity analysis using the leave-one-out cross-validation method. Additionally, we assessed potential bias by calculating the F-values of individual SNPs.

All the aforementioned methods were conducted using the TwoSampleMR package in R 4.2.1 software, with a significance level of $\alpha = 0.05$.

2.4. Identification of differentially expressed fibrosis genes

Based on the GSE197112 and GSE89632 datasets, we conducted a differential gene expression analysis using the "DESeq2" R package. The samples were divided into two groups based on the presence or absence of fibrosis, and differential gene expression between these groups was assessed using criteria of $P < 0.05$ and $|\log_2FC| > 0.585$. Subsequently, we generated volcano plots using the "ggplot2" software package to visualize the differential gene expression profiles associated with fibrosis.

2.5. Ethical statements

Human tissue samples or clinical data were not collected for this study. All data was acquired from openly accessible network

databases. The NHANES protocol has been sanctioned by the Research Ethics Review Board of the National Center for Health Statistics, and all participants have provided written informed consent.

3. Results

3.1. Population-Based study

A total of 2071 participants were included in this study (Supplementary Table S1 provides detailed information on the included data). Table 2 summarizes the characteristics of participants based on their liver fibrosis status. Among these participants, 255 (12.3 %) reported eventual liver fibrosis, with comparable prevalence rates across genders, races, marital statuses, education levels, smoking habits and alcohol consumption. In comparison to controls, individuals with liver fibrosis were more inclined to have a high BMI, a low activity level, elevated CAP, increased median liver stiffness, and higher FLI. In addition, patients with liver fibrosis showed a phenotypic aging process that significantly surpassed their chronological age.

We first analyzed the variables as continuous (PhenoageAccel = Phenotypic Age - Chronological Age) and categorical (phenotypic aging and phenotypic rejuvenation) by using the presence or absence of fibrosis as an outcome. We then constructed three multivariate logistic regression models: Model 1, unadjusted for covariates; Model 2, adjusted for age, sex, race, education, and marital status; and

Table 3.1
Association between PhenoAgeAccel and the odds of significant liver fibrosis in NHANES 2017–2020.

Variable	Model 1 OR (95 % CI) P-value	Model 2 OR (95 % CI) P-value	Model 3 OR (95 % CI) P-value
PhenoAgeAccel (years), continuous variable	1.01(1.00–1.01) P < 0.001	1.01(1.00–1.01) P < 0.001	1.01(1.00–1.01) P < 0.001
PhenoAgeAccel (years), categorical variable			
≤0 years	Ref	Ref	Ref
>0 years	1.12(1.08–1.15) P < 0.001	1.12(1.08–1.16) P < 0.001	1.08(1.05–1.12) P < 0.001

Table 3.2
Associations between PhenoAgeAccel (categorical variable) and the odds of significant liver fibrosis in MASLD based on gender, BMI, and age.

	Model 1 OR (95 % CI) P-value	Model 2 OR (95 % CI) P-value	Model 3 OR (95 % CI) P-value
Stratified by gender			
Male	1.11 (1.05–1.17) P < 0.001	1.11 (1.05–1.18) P = 0.001	1.09 (1.02–1.16) P = 0.015
Female	1.12 (1.06–1.18) P < 0.001	1.13 (1.07–1.20) P < 0.001	1.08 (1.04–1.13) P = 0.002
Stratified by BMI			
Under/normal weight	1.09 (0.93–1.27) P = 0.3	1.08 (0.94–1.24) P = 0.3	1.10 (0.94–1.28) P = 0.2
Overweight	1.01 (0.97–1.05) P = 0.6	1.00 (0.95–1.04) P = 0.9	0.99 (0.94–1.04) P = 0.7
Obese	1.13 (1.09–1.18) P < 0.001	1.14 (1.10–1.18) P < 0.001	1.14 (1.10–1.18) P < 0.001
Stratified by age (year)			
18–39	1.10 (1.03–1.17) P = 0.008	1.08 (1.02–1.15) P = 0.013	1.07 (1.01–1.14) P = 0.021
40–59	1.17 (1.10–1.24) P < 0.001	1.14 (1.08–1.21) P < 0.001	1.14 (1.07–1.22) P < 0.001
≥60	1.08 (1.00–1.17) P = 0.049	1.04 (0.95–1.14) P = 0.4	1.04 (0.94–1.14) P = 0.4

Model 3, adjusted for age, sex, race, education, marital status, activity, BMI, smoking status and alcohol consumption. When continuous variables were included in the analyses, we observed an association between phenotypic age and significant fibrosis in MASLD. The odds ratios (ORs) for Model 1, Model 2, and Model 3 were 1.01 (1.00–1.01), $P < 0.001$; 1.01 (1.00–1.01), $P < 0.001$; and 1.01 (1.00–1.01), $P < 0.001$, respectively. When categorical variables were included in the analysis, the ORs for the association of phenotypic aging with the development of liver fibrosis compared to phenotypic rejuvenation were 1.12 (1.08–1.15), $P < 0.001$; 1.12 (1.08–1.16), $P < 0.001$; and 1.08 (1.05–1.12), $P < 0.001$ (Table 3.1).

Subsequently, we conducted stratified analyses, which revealed that the association between phenotypic aging and liver fibrosis remained consistent across both males and females with similar ORs. However, when stratified by BMI and age, this association was not statistically significant in individuals who were under/normal weight, overweight, or 60 years old and above. Phenotypic aging showed a significant association with advanced fibrosis in obese individuals (OR 1.14, 95 % CI 1.10–1.18, $P < 0.001$). Notably, in young to middle-aged MASLD patients, phenotypic aging was significantly linked to advanced fibrosis (OR 1.07, 95 % CI 1.01–1.14, $P = 0.021$ and OR 1.14, 95 % CI 1.07–1.22, $P < 0.001$) (Table 3.2).

Fig. 3 illustrates the outcomes of the restricted cubic spline regression analysis depicting the correlation between PhenoAgeAccel and liver fibrosis. The curves in the figure demonstrate that when PhenoAgeAccel is greater than 1.09, it is positively associated with liver fibrosis.

3.2. MR analyses

It has been shown that a decrease in telomere length causes cellular senescence [26]. Therefore, we utilized telomere length as a marker of senescence to investigate its relationship with the progression of liver fibrosis. In Table 4, the MR analysis revealed a significant causal association between telomere length and liver fibrogenesis (IVW: OR = 0.63288, 95 % CI 0.42498–0.94249, $P = 0.02435$). Shortened telomere length was causally linked to the development of liver fibrosis. Fig. 4 visually represents the potential connection between

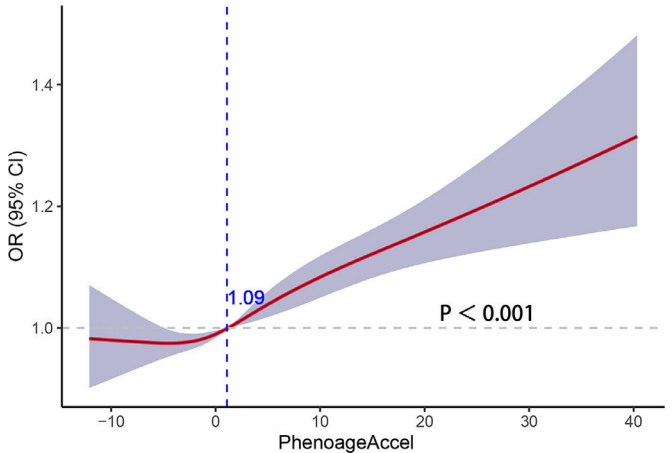


Fig. 3. Restricted cubic spline plots illustrating the correlation between phenotypic aging and liver fibrosis.

telomere length and liver fibrosis progression. We conducted an exclusion analysis and a Cochrane Q-test to evaluate the robustness of this causal relationship. The exclusion analysis indicated that none of the SNP deletions significantly impacted the observed causal link between telomere length and liver fibrogenesis. Furthermore, all Cochrane Q-tests yielded P -values above 0.05, indicating no evidence of study heterogeneity (IVW: Q-value 152.65, $P = 0.15$ and MR-Egger: Q-value 152.61, $P = 0.14$). In Supplementary Fig. S2, liver fibrosis was treated as the exposure variable and telomere length as the outcome measure, with Mendelian randomization analysis indicating no statistically significant causal relationship between them (IVW: OR = 1.00166, 95 % CI 0.99805–1.00529, $P = 0.36671$).

3.3. GEO dataset analysis and eQTL data analysis

We retrieved the GSE197112 dataset from the GEO database, which includes four normal liver samples and four liver fibrosis samples. Through a differential analysis, we identified a total of 345

Table 4
MR findings on telomere length and liver fibrosis.

Exposure	GWAS ID	nSNPs	Fibrosis and cirrhosis of liver			
			IVW method		MR-Egger	
			OR (95 % CI)	p value	OR (95 % CI)	p value
telomere length	ieu-b-4879	137	0.63288 (0.42498–0.94249)	0.02435	0.67219 (0.32965–1.37067)	0.27648

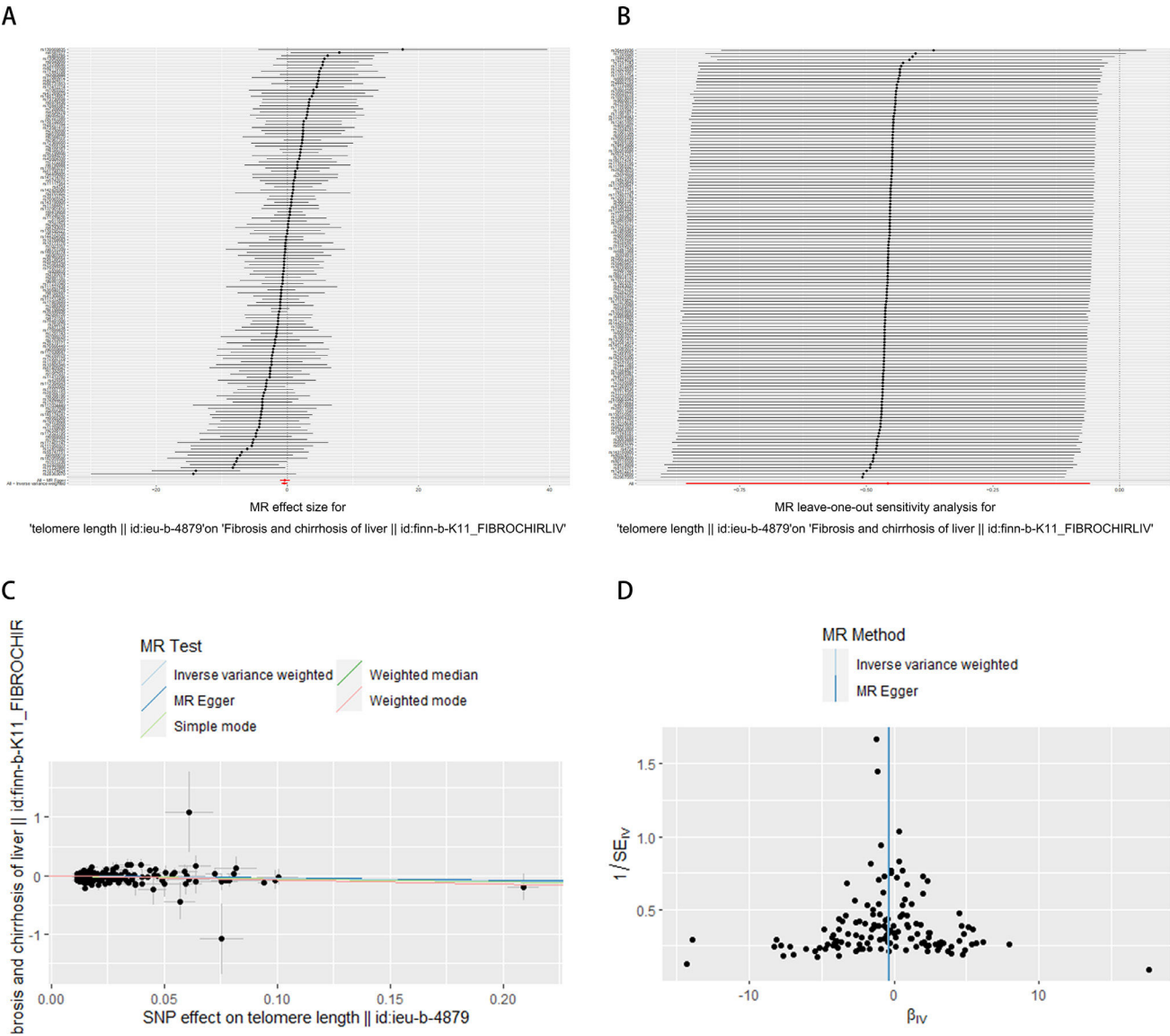


Fig. 4. Exploring the potential association between telomere length and liver fibrosis. (A) Forest plot showing the combined results of all SNPs using the IVW and MR Egger methods. Red dots represent effect estimates, and horizontal lines indicate 95 % confidence intervals. (B) Leave-one-out analysis was conducted using the IVW method. Black points represent causal effect estimates obtained by excluding single variants, while the red point denotes the inverse-variance weighted estimate using all SNPs. (C) Scatter plot illustrating the estimated effects of each Mendelian randomization method. Line slopes indicate the magnitude of the effect. (D) Funnel plot displaying estimates with all SNPs. Vertical lines represent effect estimates, demonstrating the absence of horizontal pleiotropy. IVW: inverse-variance weighted. SNP: single-nucleotide polymorphism.

differentially expressed genes, which were visualized in volcano plots (Fig. 5A). [Supplementary Table S2](#) offers comprehensive details on these significantly differentially expressed genes. After screening, we ultimately selected 26,152 SNPs from the eQTL dataset as instrumental variables. All of these SNPs satisfy the three fundamental assumptions of MR, and the F-statistics for all selected SNPs exceed 10 ([Supplementary Table S3](#) provides detailed information on the included data). Subsequently, we conducted eQTL data analysis,

identifying 453 genes associated with telomere length and 212 genes related to liver fibrosis ([Supplementary Table S4](#) provides detailed information on the data included). By utilizing Venn diagram, we identified one common gene, APOLD1, at the intersection of these gene sets (Fig. 5B). Furthermore, we performed an MR analysis on APOLD1 concerning telomere length and the incidence of liver fibrosis. The results revealed a positive correlation between changes in the APOLD1 gene and telomere length SNP variations (IVW: OR =

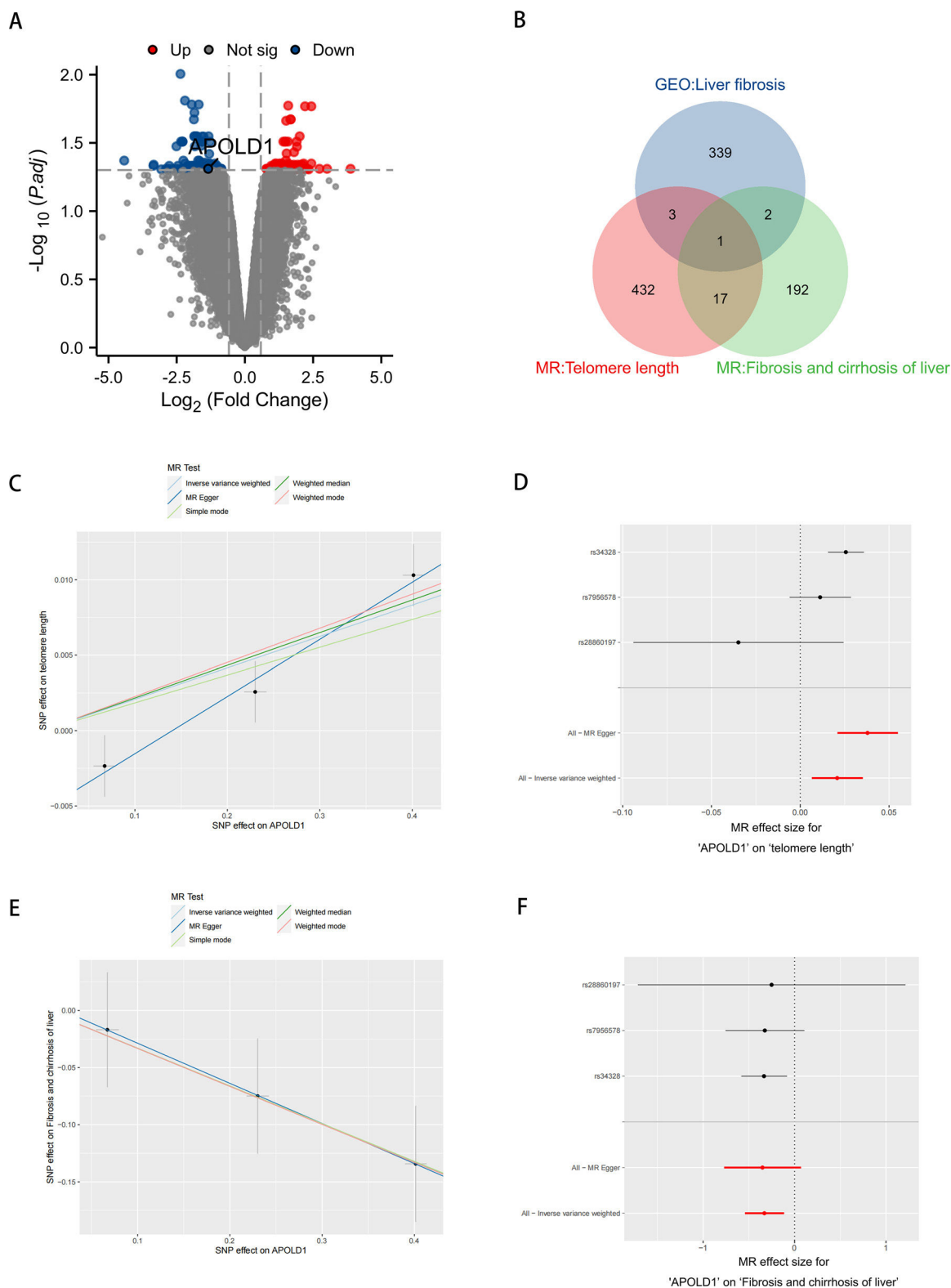


Fig. 5. Analysis of liver fibrosis and aging-related APOLD1 target acquisition. (A) GSE197112 differential gene volcano plot. (B) Venn diagram comparing telomere length eQTL genes, liver fibrosis eQTL genes, and GEO dataset. (C, E) Scatter plot illustrating the estimated effect of APOLD1 on telomere length and liver fibrogenesis. (D, F) Forest plot showing combined results of all SNPs using IVW and MR Egger methods.

1.02101, 95 % CI 1.00660–1.03563, $P = 0.00415$) (Fig. 5C and D), as well as a negative correlation between APOLD1 gene alterations and liver fibrosis SNP changes (IVW: OR = 0.71859, 95 % CI 0.58143–0.88810, $P = 0.00222$) (Fig. 5E and F). The detailed MR analysis results for APOLD1 with telomere length and liver fibrosis can be

found in [Supplementary Table S5](#). To further validate the role of APOLD1, we utilized the GSE89632 dataset to identify differentially expressed genes between liver fibrosis and healthy liver tissues, revealing significant downregulation of APOLD1 in liver fibrosis ([Supplementary Fig. S1](#) and [Supplementary Table S6](#)).

4. Discussion

This study utilized data from large observational studies and MR to explore the relationship between biological aging and the progression of MASLD to liver fibrosis. In cross-sectional studies, phenotypic aging was found to be associated with liver fibrosis (OR = 1.01; 95 % CI: 1.00–1.01, $P < 0.001$ and OR = 1.08; 95 % CI: 1.05–1.12, $P < 0.001$). Subgroup analyses indicated that phenotypic aging was significantly linked to fibrosis in obese individuals and the young to middle-aged group. Furthermore, MR analyses conducted on a European population reinforced these findings, suggesting that telomere shortening and biological aging have a causal impact on the progression of liver fibrosis. We also analyzed the GSE197112 dataset to identify differential genes associated with liver fibrosis as well as genes linked to both liver fibrosis and senescence through eQTL analysis. Subsequently, an intersection analysis was performed to pinpoint target genes that are implicated in both liver fibrosis and senescence. Finally, the expression validation was conducted using the GSE89632 dataset.

It's crucial to recognize that an increase in chronological age does not always correspond to a decline in health, and individuals of the same chronological age may exhibit significant differences in health status. Likewise, individuals of the same chronological age can show noteworthy variations in health status. Biological age, derived from biological data, serves as a more precise indicator of an organism's health and aging status compared to chronological age [27]. Phenotypic age is a composite aging score that incorporates clinical parameters and chronological age, offering a comprehensive measure of biological aging. It includes nine clinical chemistry samples reflecting various biological systems such as the liver, kidney, metabolism, inflammation, and immune function. Studies have linked PhenoAgeAccel to increased mortality from cerebrovascular disease, cancer, and diabetes [28–31]. Phenotypic age has also been correlated with the occurrence of chronic respiratory diseases [32], but its relationship with liver fibrosis remains insufficiently explored. Our analysis of NHANES data reveals a significant correlation between phenotypic age and fibrosis progression in MASLD patients, especially among obese and young to middle-aged individuals. These findings provide a reference for the use of phenotypic age as an indicator in MASLD patients, further illustrating how biological aging promotes disease progression in MASLD.

Obesity is a global pandemic, and it serves as the primary factor contributing to the development of various chronic diseases. Among these, MASLD is prevalent, affecting between 84 % to 96 % of individuals with extreme obesity [33]. This underscores the direct relationship between obesity and MASLD, highlighting how excessive weight can significantly increase the risk and prevalence of this liver condition [34]. Excessive obesity leads to adipocyte hyperplasia, apoptosis, necrosis, and fibrosis, culminating in cirrhosis and hepatocellular carcinoma [35]. In obesity, changes in the structure and function of the gut microbiota lead to dysbiosis, potentially causing excessive activation of liver immune cells. This process can result in inflammation, fibrosis, and liver damage associated with MASLD [36,37]. Additionally, obesity induces chronic low-grade inflammation and increased oxidative stress, accelerating the aging process. It also affects key aging-related signaling pathways, such as insulin/IGF-1, mTOR, and AMPK, which are crucial for maintaining metabolic health and delaying aging. Moreover, obesity has been reported to accelerate telomere shortening, promoting cellular senescence [38]. Similar to our findings, our subgroup analysis revealed that biological aging was more likely to promote the progression of MASLD to liver fibrosis in obese patients. In the adolescent population, higher metabolic rates and robust physiological recovery may shorten the duration of disease manifestation, reducing the impact of phenotypic age on the progression of MASLD. Conversely, in the elderly, the occurrence of multiple chronic diseases and biological changes complicates the correlation between phenotypic aging and MASLD development [39].

Therefore, the relationship between phenotypic age and MASLD progression is most pronounced in the young to middle-aged adult population. We hypothesized that anti-aging therapy may have a more pronounced effect on young to middle-aged, obese MASLD patients. The mechanisms underlying these findings need to be further elucidated.

The aging process is reflected in molecular markers associated with epigenetics, transcriptomics, and telomere length. Therefore, these markers provide valuable insights into an individual's biological age. Telomere disorders often lead to inflammation and fibrosis in the liver, suggesting their potential impact on liver disease [40]. Using MR, we investigated the causal link between telomere length and liver fibrosis. Our study establishes a clear causal connection between telomere shortening and liver fibrosis, providing key evidence for the association between progression of biological aging and liver fibrosis.

In this study, we conducted a comprehensive analysis by integrating data from disease GWAS and eQTL to identify novel therapeutic targets for liver fibrosis and senescence. Initially, we identified differentially expressed genes related to fibrosis from the dataset GSE197112. Subsequently, we cross-referenced telomere length-related genes and liver fibrosis-related genes using telomere length GWAS data and eQTL data. Through these analyses, we identified APOLD1 as a key candidate. The identification of APOLD1 marks a significant advancement in our understanding of liver fibrosis and senescence, offering promising avenues for future therapeutic interventions. APOLD1, also known as the early vascular response gene, is a gene that is specifically expressed in endothelial cells in response to various stimuli such as ischemia, cytokines, growth factors, and stress [41]. The selective expression of genes in endothelial cells plays a crucial role in controlling thrombus formation. Studies have demonstrated that in mice lacking APOLD1 gene expression, levels of procoagulant proteins such as tissue factor (TF) increase in the arterial wall. TF can trigger the activation of the coagulation cascade, contributing to the aggravation of arterial thrombosis. Further, recent research has indicated that silencing APOLD1 in human endothelial cells disrupts the interface between cell junctions and the cytoskeleton [42]. Disruptions between cellular connectivity and the cytoskeleton can distort intercellular signaling and cause structural changes within cells, contributing to the initiation and progression of fibrosis [43,44]. Additionally, any imbalance in intravascular homeostasis is closely associated with the aging process [45]. Our study similarly elucidated the role of APOLD1 in fibrosis. We proposed that APOLD1 is intricately linked to both liver fibrosis and aging, suggesting it as a promising target for therapeutic intervention in liver fibrosis.

This study is the first to establish a link between biological aging and the development of liver fibrosis through comprehensive analyses, including NHANES analysis, MR analysis, and eQTL analysis. Notably, the findings from the NHANES analysis indicating that phenotypic aging promotes liver fibrosis, along with the MR analysis showing that telomere shortening contributes to liver fibrosis, and the set of genes causally linked to both telomere shortening and liver fibrosis identified through eQTL analysis, culminating in the identification of APOLD1 through integration with GSE197112 differential gene expression data. Furthermore, APOLD1 expression was validated using GSE89632. Collectively, these results strengthen the conclusions drawn from our study.

This research not only highlights the correlation between aging and liver fibrosis, offering a clinically relevant indicator of aging, but also identifies a potential gene target for future therapeutic interventions. However, the study does come with certain limitations. Primarily, being database-driven, its generalizability is limited by the predominantly European-American ancestry of the datasets used. Extending these findings to other racial groups would necessitate additional research and validation to ensure broader relevance. Furthermore, while potential molecular targets have been identified in

this study, their efficacy in a clinical context remains uncertain. Subsequent experimental validation and clinical trials are imperative to validate the therapeutic potential of the identified targets.

5. Conclusions

In conclusion, our study establishes phenotypic age as a significant independent predictor of liver fibrosis in the MASLD population, utilizing data from the NHANES database. Particularly noteworthy is the heightened significance of this association among young to middle-aged obese MASLD patients. This underscores the pivotal role of phenotypic age in identifying individuals at elevated risk for liver fibrosis, urging physicians to closely monitor MASLD patients. Furthermore, we highlight the *APOLD1* gene as a potential target for future therapeutic interventions. While our findings illuminate novel avenues for managing this condition, further investigations are imperative to validate these discoveries.

Author contributions

Jiaxin Zhao contributed to the Conceptualization, Data curation, Formal analysis, Methodology, and Writing - original draft. Jiaxin Zhao and Huiying Zhou performed Investigation and Interpretation of data. Jiaxin Zhao and Rui Wu contributed significantly to the Formal analysis and Writing - original draft. Jiaxin Zhao performed the Data curation and Data analysis, and wrote the manuscript (Writing - original draft). Jiaxin Zhao, Chen Ruan, Cheng Wang, Jiawei Ding, and Tao Zhang helped perform the Investigation with constructive discussions. Jiaxin Zhao, Zheyu Fang, Huilin Zheng, Lei Zhang, Jie Zhou, and Zhenhua Hu helped Writing - review & editing and revised the manuscript critically. All authors reviewed and approved the final version of the manuscript (Writing - review & editing).

Funding

This study was supported by [National Key R&D Program of China \(2022YFA1104600\)](#), Key Science and Technology Program of Zhejiang Province (No. [WKJ-ZJ-1818](#)).

Declaration of interests

None.

Acknowledgments

The authors acknowledge all the clinical and research staff from the research centers.

Supplementary materials

Supplementary material associated with this article can be found in the online version at [doi:10.1016/j.aohep.2024.101579](https://doi.org/10.1016/j.aohep.2024.101579).

References

- [1] Makri E, Goulas A, Polyzos SA. Epidemiology, pathogenesis, diagnosis and emerging treatment of nonalcoholic fatty liver disease. *Arch Med Res* 2021;52(1):25–37.
- [2] Younossi ZM, et al. Diagnostic modalities for nonalcoholic fatty liver disease, non-alcoholic steatohepatitis, and associated fibrosis. *Hepatology* 2018;68(1):349–60.
- [3] Rinella ME, et al. A multisociety Delphi consensus statement on new fatty liver disease nomenclature. *Ann Hepatol* 2024;29(1):101133. <https://doi.org/10.1016/j.aohep.2023.101133>.
- [4] Targher G, Byrne CD, Tilg H. NAFLD and increased risk of cardiovascular disease: clinical associations, pathophysiological mechanisms and pharmacological implications. *Gut* 2020;69(9):1691–705.
- [5] Chen Y, et al. Aging reprograms the hematopoietic-vascular niche to impede regeneration and promote fibrosis. *Cell Metab* 2021;33(2):395–410 e4.
- [6] Levine ME, et al. An epigenetic biomarker of aging for lifespan and healthspan. *Aging (Albany NY)* 2018;10(4):573–91.
- [7] Tanaka T, et al. Plasma proteomic signature of age in healthy humans. *Aging Cell* 2018;17(5):e12799.
- [8] Liu Z, et al. A new aging measure captures morbidity and mortality risk across diverse subpopulations from NHANES IV: a cohort study. *PLoS Med* 2018;15(12):e1002718.
- [9] Graf GH, et al. Testing Black–White disparities in biological aging among older adults in the united states: analysis of DNA-methylation and blood-chemistry methods. *Am J Epidemiol* 2022;191(4):613–25.
- [10] Gao X, et al. Accelerated biological aging and risk of depression and anxiety: evidence from 424,299 UK Biobank participants. *Nat Commun* 2023;14(1):2277.
- [11] Blackburn EH, Gall JG. A tandemly repeated sequence at the termini of the extra-chromosomal ribosomal RNA genes in *Tetrahymena*. *J Mol Biol* 1978;120(1):33–53.
- [12] López-Otin C, et al. The hallmarks of aging. *Cell* 2013;153(6):1194–217.
- [13] Smith GD, Ebrahim S. Mendelian randomization: can genetic epidemiology contribute to understanding environmental determinants of disease? *Int J Epidemiol* 2003;32(1):1–22.
- [14] Zhu Z, et al. Integration of summary data from GWAS and eQTL studies predicts complex trait gene targets. *Nat Genet* 2016;48(5):481–7.
- [15] Castera L, Friedrich-Rust M, Loomba R. Noninvasive assessment of liver disease in patients with nonalcoholic fatty liver disease. *Gastroenterology* 2019;156(5):1264–81 e4.
- [16] Pu K, et al. Diagnostic accuracy of controlled attenuation parameter (CAP) as a non-invasive test for steatosis in suspected non-alcoholic fatty liver disease: a systematic review and meta-analysis. *BMC Gastroenterol* 2019;19(1):51.
- [17] Bedogni G, et al. The fatty liver index: a simple and accurate predictor of hepatic steatosis in the general population. *BMC Gastroenterol* 2006;6:33.
- [18] Karlas T, et al. Individual patient data meta-analysis of controlled attenuation parameter (CAP) technology for assessing steatosis. *J Hepatol* 2017;66(5):1022–30.
- [19] Lee H, et al. Metabolic dysfunction-associated fatty liver disease and incident cardiovascular disease risk: a nationwide cohort study. *Clin Gastroenterol Hepatol* 2021;19(10):2138–47 e10.
- [20] Grundy SM, et al. Diagnosis and management of the metabolic syndrome: an American Heart Association/National Heart, Lung, and Blood Institute scientific statement: executive summary. *Crit Pathw Cardiol* 2005;4(4):198–203.
- [21] Xiao G, et al. Comparison of laboratory tests, ultrasound, or magnetic resonance elastography to detect fibrosis in patients with nonalcoholic fatty liver disease: a meta-analysis. *Hepatology* 2017;66(5):1486–501.
- [22] Eddowes PJ, et al. Accuracy of FibroScan controlled attenuation parameter and liver stiffness measurement in assessing steatosis and fibrosis in patients with nonalcoholic fatty liver disease. *Gastroenterology* 2019;156(6):1717–30.
- [23] Argalia G, et al. Comparison of point shear wave elastography and transient elastography in the evaluation of patients with NAFLD. *Radiol Med* 2022;127(5):571–6.
- [24] Sultanik P, et al. Prevalence and prognosis of patients with MASLD-related cirrhosis after an ICU hospitalization in France: a single-centre prospective study. *Aliment Pharmacol Ther* 2024;60(6):796–810.
- [25] Vösa U, et al. Large-scale cis- and trans-eQTL analyses identify thousands of genetic loci and polygenic scores that regulate blood gene expression. *Nat Genet* 2021;53(9):1300–10.
- [26] Aubert G, Lansdorp PM. Telomeres and aging. *Physiol Rev* 2008;88(2):557–79.
- [27] Lowsky DJ, et al. Heterogeneity in healthy aging. *J Gerontol A Biol Sci Med Sci* 2014;69(6):640–9.
- [28] Kong L, et al. Genetic evidence for causal effects of socioeconomic, lifestyle, and cardiometabolic factors on epigenetic-age acceleration. *J Gerontol A Biol Sci Med Sci* 2023;78(7):1083–91.
- [29] Ma Z, et al. Association between biological aging and lung cancer risk: cohort study and Mendelian randomization analysis. *iScience* 2023;26(3):106018.
- [30] Mak JKL, et al. Clinical biomarker-based biological aging and risk of cancer in the UK Biobank. *Br J Cancer* 2023;129(1):94–103.
- [31] Li X, et al. Accelerated aging mediates the associations of unhealthy lifestyles with cardiovascular disease, cancer, and mortality. *J Am Geriatr Soc* 2024;72(1):181–93.
- [32] Wang T, et al. Associations of combined phenotypic ageing and genetic risk with incidence of chronic respiratory diseases in the UK Biobank: a prospective cohort study. *Eur Respir J* 2024;63(2):2301720.
- [33] Meneses D, et al. Prevalence and predictors of non-alcoholic steatohepatitis in patients with morbid obesity. *Endocrinol Diabetes Nutr (Engl Ed)* 2022;69(3):178–88.
- [34] Mathews SE, Kumar RB, Shukla AP. Nonalcoholic steatohepatitis, obesity, and cardiac dysfunction. *Curr Opin Endocrinol Diabetes Obes* 2018;25(5):315–20.
- [35] Gutiérrez-Cuevas J, Santos A, Armendariz-Borunda J. Pathophysiological molecular mechanisms of obesity: a link between MAFLD and NASH with cardiovascular diseases. *Int J Mol Sci* 2021;22(21):11629.
- [36] Zazueta A, et al. Alteration of gut microbiota composition in the progression of liver damage in patients with metabolic dysfunction-associated steatotic liver disease (MASLD). *Int J Mol Sci* 2024;25(8):4387.
- [37] Portincasa P, et al. Gut microbes in metabolic disturbances. Promising role for therapeutic manipulations? *Eur J Intern Med* 2024;119:13–30.
- [38] Santos AL, Sinha S. Obesity and aging: molecular mechanisms and therapeutic approaches. *Ageing Res Rev* 2021;67:101268.
- [39] He QJ, et al. Recent advances in age-related metabolic dysfunction-associated steatotic liver disease. *World J Gastroenterol* 2024;30(7):652–62.

- [40] Savage SA, Bertuch AA. The genetics and clinical manifestations of telomere biology disorders. *Genet Med* 2010;12(12):753–64.
- [41] Aboyans V, Mazzolai L. The ESC working group on aorta & peripheral vascular diseases. *Eur Heart J* 2020;41(44):4221–3.
- [42] Stritt S, et al. APOLD1 loss causes endothelial dysfunction involving cell junctions, cytoskeletal architecture, and Weibel–Palade bodies, while disrupting hemostasis. *Haematologica* 2023;108(3):772–84.
- [43] Pankonien I, et al. CFTR, cell junctions and the cytoskeleton. *Int J Mol Sci* 2022;23(5):2688.
- [44] Resnikoff HA, Miller CG, Schwarzbauer JE. Implications of fibrotic extracellular matrix in diabetic retinopathy. *Exp Biol Med (Maywood)* 2022;247(13):1093–102.
- [45] Grunewald M, et al. Counteracting age-related VEGF signaling insufficiency promotes healthy aging and extends life span. *Science* 2021;373(6554):abc8479.